



Cycling Performance of Supercapacitors Assembled with Polypyrrole/Multi-Walled Carbon Nanotube/Conductive Carbon Composite Electrodes

Santhosh Paul, Jae-Hong Kim, and Dong-Won Kim[†]

Department of Chemical Engineering, Hanyang University, Seungdong-Gu, Seoul 133-791, Republic of Korea

ABSTRACT:

Polypyrrole (PPy)/multi-walled carbon nanotube (MWCNT)/conductive carbon (CC) composites are synthesized by the chemical oxidative polymerization method. The morphology analysis of the composite materials indicates uniform coating of PPy over MWCNTs and conductive carbon. The electrochemical performances of PPy/MWCNT/CC composites with different compositions are evaluated in order to optimize the composition of the composite electrode. Galvanostatic charge-discharge measurements and electrochemical impedance spectroscopy studies prove the excellent cycling stability of the PPy/MWCNT/CC composite electrodes.

Keywords: Carbon nanotube, Composite electrode, Electrochemical capacitor, Polypyrrole, Supercapacitor

Received May 6, 2011 : Accepted June 8, 2011

1. Introduction

Supercapacitors have attracted great attention as promising energy storage devices due to their high specific power and long cycle life.^{1,2)} High-surface carbons, redox metal oxides and conducting polymers are the main families of electrode materials being studied for supercapacitor applications.^{3,4)} Among them, ruthenium oxides and conducting polymers have been shown to deliver higher specific capacitance than carbon materials, since they store charge through both double-layer and redox capacitive mechanisms. Since the conducting polymers cost less than ruthenium oxides, they have received much attention as electrode materials. A wide variety of conducting polymers - such as polyaniline (PANI),⁵⁻⁸⁾ polypyrrole (PPy),⁹⁻¹²⁾ polyethylenedioxythiophene,^{13,14)} polythiophene and its substituted counterparts^{15,16)} - have been studied for supercapacitor applications. Of these, PANI and PPy have been considered the most promising materials

for supercapacitor applications due to their high specific capacitance, easy synthesis, high conductivity and low cost. However, the main drawback of conducting polymers is poor cycle life due to the volume change during the doping and dedoping processes, which leads to degradation of the polymer electrode during cycling. Hence, it is necessary to strengthen the electrochemically active sites of conducting polymers by the addition of large surface area carbon materials or carbon nanotubes (CNTs). CNTs are attractive materials for electrodes of electrochemical energy storage devices due to their highly accessible surface area, high electronic conductivity and mechanical stability. There have been many investigations of the electrochemical performance of different kinds of conducting polymer/CNT composite electrodes for supercapacitor applications.¹⁷⁻²⁶⁾ However, the long-term cycleability of supercapacitors assembled with them is not enough for practical application, compared to that of electric double layer capacitors with activated carbon materials.

With the aim of improving the cycleability of the PPy-based electrodes, we synthesized PPy/multi-walled carbon nanotube (MWCNT)/conductive carbon (CC) composites.

[†]Corresponding author. Tel.: +82-2-2220-2337
E-mail address: dongwonkim@hanyang.ac.kr

In this study, the electrochemical properties of the nano-composite electrodes were investigated by cyclic voltammetry, galvanostatic charge-discharge cycles and electrochemical impedance spectroscopy. The effect of the composition of composite electrodes on the electrochemical performance of the cells was also investigated.

2. Experimental

2.1. Synthesis of PPy/MWCNT/CC composites

Pyrrole, anhydrous ferric chloride (FeCl_3), polyvinyl pyrrolidone (PVP), polytetrafluoroethylene (PTFE), isopropanol (IPA), N-methylpyrrolidone (NMP) and potassium chloride (KCl) were purchased from Aldrich chemicals. The pyrrole monomer was purified before use and the rest of the chemicals were used as received. The MWCNT was purchased from Hanwha Nanotech, which has been prepared by a chemical vapor deposition. The PPy/MWCNT/CC composites were synthesized by the conventional oxidative chemical polymerization method using anhydrous FeCl_3 .²⁷⁾ MWCNTs were used as templates for the PPy to grow over them, and conductive carbon powder (Super-P) was also added *in situ* in order to improve the overall conductivity of the composite material. The advantage of adding conductive carbon into the polymerization system is that it can be coated with PPy, thus exposing more effective surface area of the active electrode material without any reduction in the bulk electronic conductivity of the composites. In a typical synthesis procedure, an adequate amount of MWCNTs and Super-P were stirred vigorously in 0.14 M aqueous FeCl_3 solution. This suspension was sonicated for 3 h to facilitate the dispersion of MWCNTs and Super-P. 500 mL pyrrole was added very slowly and by the drop into 100 mL stirring solution, and the polymerization continued for another 4 h. The precipitated composite material was then filtered and washed very well with water and methanol. It was vacuum dried at 70°C overnight and stored in a desiccator. Three composite electrodes with different compositions were synthesized by varying the content of MWCNTs between 10 (PPy/MWCNT-10/CC), 15 (PPy/MWCNT-15/CC), and 20 wt% (PPy/MWCNT-20/CC) of the total weight of the composite material by keeping the same quantity of Super-P content (20 wt%) in all compositions.

2.2. Cell assembly and measurements

A slurry of the composite material was made with a mixture of PTFE/PVP binders in order to achieve good

adhesion on Ti foil. The excellent wetting and adhesive film formation properties of PVP are well known and thus a proper amount of PVP was also added along with PTFE as a binder. The binder materials (PTFE/PVP) in the weight ratio of 7 : 3 were first dissolved in an IPA/NMP mixed solvent and then PPy/MWCNT/CC composite material was added into the polymer binder solution. The solution was sonicated for 1 h and ball-milled for another 15 h in order to make homogenous slurry. The weight ratio of composite to binder was maintained at 90 : 10. The resultant slurry was cast onto Ti foil using a doctor blade. The electrodes were dried in a vacuum oven at 80°C for 24 h and roll-pressed to enhance particulate contact and adhesion to the foils. Sandwich-type cells were assembled with two symmetric PPy/MWCNT/CC composite electrodes (area : 1.0 cm^2). The electrolyte used to assemble the cell was a 1.0 M KCl aqueous electrolyte solution with a paper separator (thickness : 40 μm , Nippon Kodoshi Co.). Both the electrodes and separator were soaked in the electrolyte before cell assembly. The symmetrical cell was enclosed in a metallized plastic bag and vacuum-sealed. The morphologies of the composite materials were examined using field emission scanning electron microscopy (FESEM, JEOL JSM-6701). Cyclic voltammograms (CVs) were recorded from 0 to 0.6 V at different scan rates. AC impedance measurements were performed on CH Instruments in the frequency range of 0.1 Hz~100 kHz with an ac perturbation of 10 mV. Galvanostatic charge-discharge cycling of the cell was conducted over voltage ranges of 0 to 0.6 V with battery-test equipment at constant current densities from 0.5 to 10 mA cm^{-2} at room temperature.

3. Results and discussion

The FESEM images of pristine MWCNTs, conductive carbon and various PPy/MWCNT/CC composites are shown in Fig. 1. From the images of composites in Fig. 1 (c)-(e), it can be seen that MWCNTs and conductive carbon are evenly coated by the PPy layer. For PPy/MWCNT-10/CC composite, the measured diameters for nanotubes and globular carbon material are around 80 and 120 nm, respectively. The diameters of both materials in the composite almost doubled compared to those of the corresponding pristine materials. The thickness of the PPy layer on carbon substrate decreases as the content of MWCNT in the composite increases. A very thin coating layer of PPy on MWCNT and conductive carbon can be observed in the PPy/MWCNT-20/CC composite. In

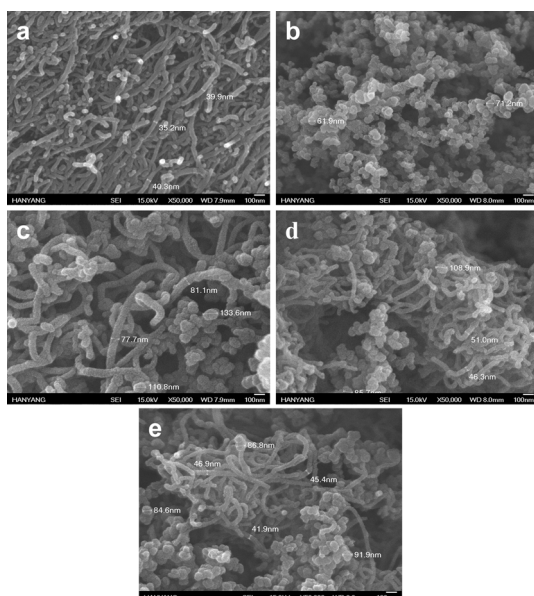


Fig. 1. FESEM images of (a) pristine MWCNTs, (b) Super-P, (c) PPy/MWCNT-10/CC composite, (d) PPy/MWCNT-15/CC composite and (e) PPy/MWCNT-20/CC composite.

these composites, MWCNTs and conductive carbon can offer good mechanical support to PPy and also ensure good electronic conduction in the electrode when the polymer is even in an insulating state.

The electrochemical properties of the composite electrode material were investigated by the CVs of the two-electrode cells assembled with the same electrode. In the literature, the specific capacitance calculated from the three-electrode cell for the PPy-based electrodes was always quoted higher than that obtained for a symmetric two-electrode cell.¹⁹⁾ In our study, the evaluation of specific capacitance for the composite electrode was performed in a real supercapacitor, constituted by a two-electrode cell. The voltammograms obtained for the PPy/MWCNT-15/CC composite electrode at different scan rates are presented in Fig. 2. The CVs obtained for the other two composite electrodes also followed the similar behavior. The CVs of the composite electrode look almost rectangular with good symmetry at all scan rates, showing highly efficient capacitive behavior with good charge propagation. The shape of CVs obtained in the PPy/MWCNT-15/CC electrode is very similar to that of PPy/CNT composite electrodes reported in the literature.^{18-20, 23-25)} The voltage reversal at the potential limit is very fast, which indicates a fast charge and discharge behavior of the cell. Current value is found to increase with increasing scan rate, as expected. The CVs are very stable

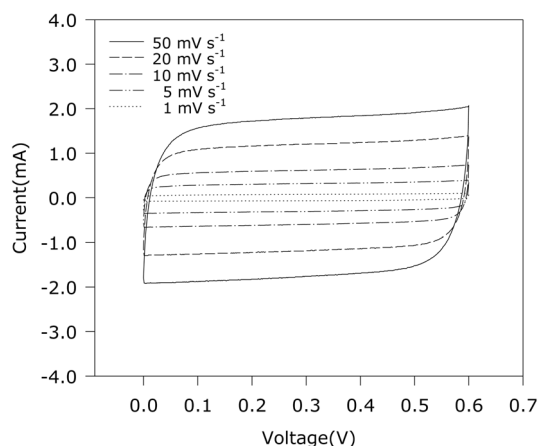


Fig. 2. Cyclic voltammograms obtained for the symmetric two-electrode cell assembled with PPy/MWCNT-15/CC composite. (electrolyte : 1.0 M KCl)

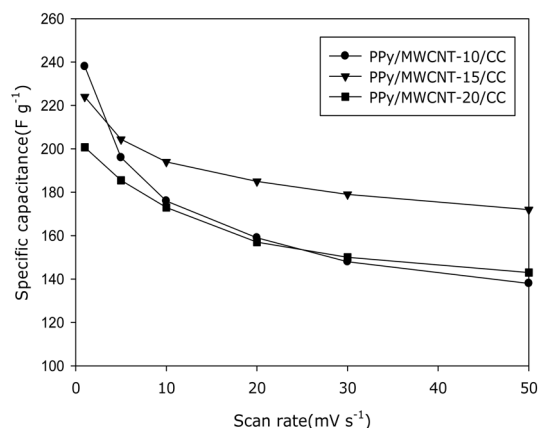


Fig. 3. Specific capacitance obtained for different composite electrodes with respect to scan rates in two-electrode cells.

and unchanged through cycling, which indicates good cycleability of the electrochemical reaction. The specific capacitance of the single-compartment electrode was calculated by integrating the total area under the voltammogram, as reported previously.²⁸⁾ Fig. 3 shows a comparison of the specific capacitances obtained for three composite electrodes in the symmetrical cell configuration as a function of scan rate. At a low scan rate (1 mV s^{-1}), the specific capacitance of PPy/MWCNT/CC electrodes ranged from 200.7 to 238.0 F g^{-1} based on weight of active materials in one electrode, and the values increased with increasing PPy content. An increase in the specific capacitance of PPy/MWCNT/CC composite with increasing PPy content can be associated with pseudo capacitance contributed by PPy. It is noteworthy that pure MWCNT has a low specific

capacitance not exceeding 40 F g^{-1} . Hence, taking into account that the content of MWCNTs in the composite is less than 20 wt%, the total capacitance is mainly due to the PPy. All of the electrodes exhibited a decrease in specific capacitance with increasing scan rate. The PPy/MWCNT-15/CC composite electrode showed better rate capability than the other two composite electrodes. In the PPy/MWCNT-15/CC composite electrode, MWCNTs and conductive carbon are evenly and thinly coated by high capacitive PPy, which produces a porous three-dimensional network of the composites supported by the nano-sized MWCNT and conductive carbon. It can provide a large surface area of PPy for electrolyte access and high electronic conductivity of carbon materials.

The symmetric cell assembled with the PPy/MWCNT-15/CC composite electrode was subjected to charge-discharge cycling in the voltage range of 0 to 0.6 V at a constant current of 0.5 mA cm^{-2} , and its charge-discharge curves are shown in Fig. 4. The charge-discharge curves exhibit a well-behaved triangular wave with no curvature and there is no large IR drop even in the last cycle, which indicates the prominent capacitive behavior of the cell. The cell shows good cycling stability without diminishing the charging or discharging times during 500 cycles. This result demonstrates that the PPy/MWCNT/CC composite electrode has high stability for a long cycle life. The specific capacitance of the electrode was calculated using the formula $C (\text{F g}^{-1}) = 2 It / (m \Delta E)$, where I is the current applied for the charging and discharging, t is the time of discharge, ΔE is the voltage difference between the upper and lower potential limit, and m is the mass of active

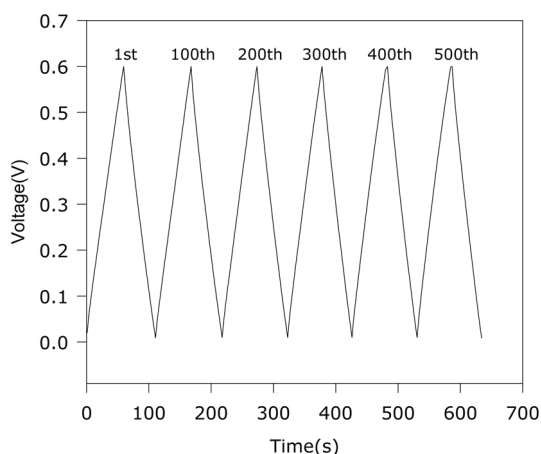


Fig. 4. Charge and discharge curves of the symmetric cell assembled with PPy/MWCNT-15/CC composite electrode.

materials (PPy and MWCNT) in one of the electrodes. The factor of 2 arises because the total capacitance measured from the cell is the addition of two equivalent single electrode capacitors in series.¹⁹⁾ The specific capacitance of the cells as a function of cycle number is presented in Fig. 5. The initial specific capacitances obtained from the galvanostatic charge-discharge measurements range from 150.0 to 183.7 F g^{-1} , and increase with increasing PPy content. This trend is consistent with the results obtained from CVs of the two-electrode cells. The loss of capacitance is very small during the charge and discharge cycles. The excellent cycle life of the cells assembled with the PPy/MWCNT/CC composite can be ascribed to the electrochemical and mechanical stability of active sites on PPy, achieved by the addition of carbon nanotubes and conductive carbon with large surface area.

Rate capabilities of cells assembled with PPy/MWCNT/CC electrodes were evaluated with varying current densities from 0.5 to 10 mA cm^{-2} , which are shown in Fig. 6. The capacitance of the cells decreased as the current densities increased, due to the internal resistance of the electrodes. The cell assembled with PPy/MWCNT-15/CC shows the highest capacitance at high current rates among the cells studied in this work. On the other hand, the decrease in specific capacitance is prominent in the PPy/MWCNT-10/CC composite-based cell. These results are consistent with those obtained from CV results, as explained in Fig. 3. The reduction of capacitance in the PPy/MWCNT-10/CC-based cell at high current rates may be associated with the high thickness of the PPy layer, which gives high internal resistance of the cell. In the case of the PPy/

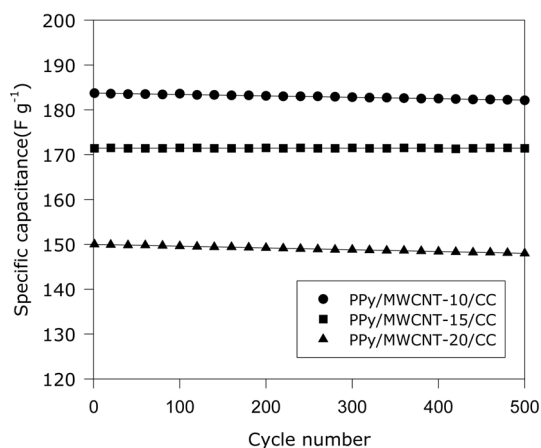


Fig. 5. Specific discharge capacitance as a function of cycle number for the cells assembled with three different composite electrodes, obtained at a constant current density of 0.5 mA cm^{-2} .

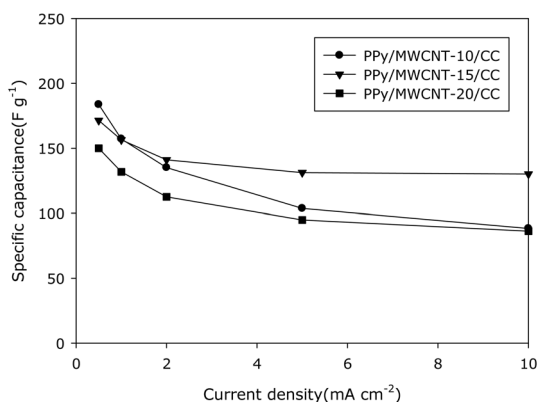


Fig. 6. Specific capacitance as a function of current density for the cells assembled with different PPy/MWCNT/CC composites.

MWCNT-20/CC electrode, the amount of PPy is not enough for the complete coverage of MWCNT or conductive carbon. Thus, the high rate-specific capacitance of the cell constructed with this particular composite is not as high as that of the cell assembled with PPy/MWCNT-15/CC.

To gain some insight into the electrochemical behavior of the PPy/MWCNT/CC composite electrodes, ac impedance of the cells was measured. Fig. 7(a) and (b) present ac impedance spectra of the cells before and after 500 cycles in the voltage range of 0 to 0.6 V. All of the impedance measurements were made for the cells in their discharged state without applying any external potential. In all three spectra obtained before and after cycling, the cells displayed a semicircle, followed by a capacitive spike. High-frequency intercepts of the real axis, which are related to the electrolyte resistances, are almost the same among the three cells. The semicircle that appeared in the middle-to-low frequency region is related to the charge transfer reaction occurring in the cells. Before cycling, charge transfer resistances calculated from these spectra are 7.4, 2.1, and 4.3 Ω for the cells assembled with PPy/MWCNT-10/CC, PPy/MWCNT-15/CC, and PPy/MWCNT-20/CC, respectively. The lowest value of charge transfer resistance in the cell with the PPy/MWCNT-15/CC electrode can be ascribed to the large surface area that allows excellent electrolyte access and provides low internal resistance. It suggests that the introduction of proper content of MWCNTs and conductive carbon into the composite may facilitate the charge transfer and reduce the internal resistance of the electrode. At low frequencies, the ac impedance spectra exhibited a slightly tilted vertical line of a limiting diffusion process, which was a characteristic feature of pure capacitive behavior.²⁹⁾ The ac impedance spectra

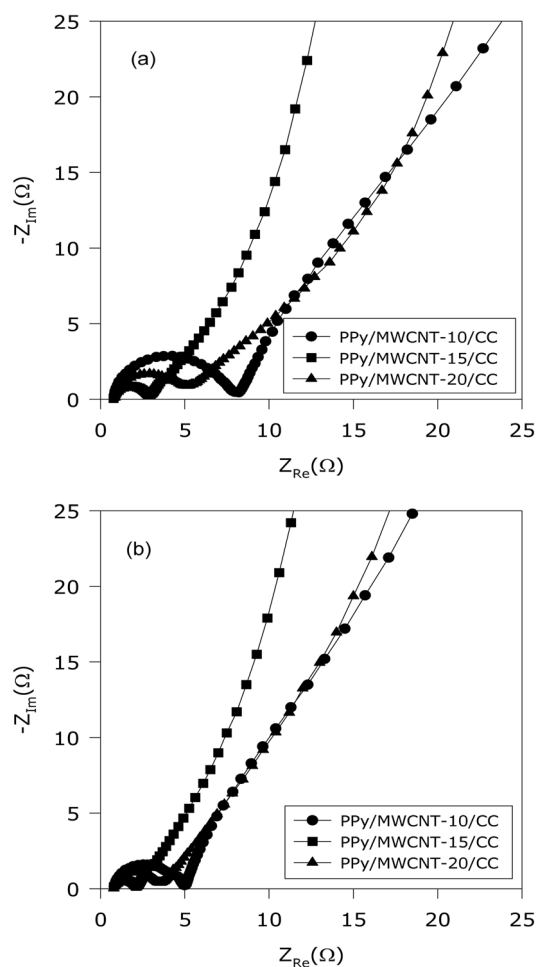


Fig. 7. AC impedance spectra of the cells assembled with different PPy/MWCNT/CC composites : (a) before cycling and (b) after 500 cycles in the voltage range of 0-0.6 V.

obtained after 500 cycles also followed the same trend as the spectra obtained before cycling. It should be noted that the charge transfer resistance values are reduced for all of the cells after 500 cycles, as shown in Fig. 7(b). This result suggests that the PPy/MWCNT/CC composite electrodes are very stable without degradation under the repeated charge and discharge cycles.

4. Conclusions

The PPy/MWCNT/CC composites with varying content of MWCNTs were synthesized and characterized for supercapacitor applications. The specific capacitance increased with increasing PPy content in the composite.

The cells assembled with PPy/MWCNT-15/CC composite electrodes exhibited good rate capability and excellent cycle life. Low internal resistance in the cells was proved by electrochemical impedance spectroscopy after charge-discharge cycles. From these results, the PPy/MWCNT/CC composites with optimum composition can be considered promising electrode material with high capacitance and long cycle life in the application of supercapacitors.

Acknowledgements

This work is the outcome of the Manpower Development Program for Energy & Resources supported by the Ministry of Knowledge and Economy (MKE). This research was also supported by a Grant from the Fundamental R&D Program for Core Technology of Materials, funded by the Ministry of Knowledge Economy, Korea

References

1. B.E. Conway, *J. Electrochem. Soc.*, **138**, 1539 (1991).
2. A.S. Arico, P. Bruce, B. Scrosati, J.M. Tarascon and W.V. Schalkwijk, *Nat. Mater.*, **4**, 366 (2005).
3. A. Burke, *J. Power Sources*, **91**, 37 (2000).
4. R. Kotz and M. Carlen, *Electrochim. Acta*, **45**, 2483 (2000).
5. D. Belanger, X. Ren, J. Davey, F. Uribe, and S. Gottesfeld, *J. Electrochem. Soc.*, **147**, 2923 (2000).
6. K.S. Ryu, K.M. Kim, N.G. Park, Y.J. Park and S.H. Chang, *J. Power Sources*, **103**, 305 (2002).
7. K.R. Prasad and N. Munichandraiah, *J. Power Sources*, **112**, 443 (2002).
8. B.C. Kim, J.S. Kwon, J.M. Ko, J.H. Park, C.O. Too and G.G. Wallace, *Synth. Met.*, **160**, 94 (2010).
9. K. Jurewicz, S. Delpeux, V. Bertagna, F. Beguin and E. Frackowiak, *Chem. Phys. Lett.*, **347**, 36 (2001).
10. J.H. Park, J.M. Ko, O.O. Park and D.W. Kim, *J. Power Sources*, **105**, 20 (2002).
11. M.D. Ingram, H. Staesche and K.S. Ryder, *Solid State Ionics*, **169**, 51 (2004).
12. L.Z. Fan and J. Maier, *Electrochem. Commun.*, **8**, 937 (2006).
13. K.S. Ryu, Y.G. Lee, Y.S. Hong, Y.J. Park, X. Wu, K.M. Kim, M.G. Kang, N.G. Park and S.H. Chang, *Electrochim. Acta*, **50**, 843 (2004).
14. K. Lota, V. Khomenko and E. Frackowiak, *J. Phys. Chem. Solids*, **65**, 295 (2004).
15. C. Arbizzani, M.C. Gallazzi, M. Mastragostino, M. Rossi and F. Soavi, *Electrochem. Commun.*, **3**, 16 (2001).
16. M. Mastragostino, C. Arbizzani and F. Soavi, *Solid State Ionics*, **148**, 493 (2002).
17. K.H. An, K.K. Jeon, J.K. Heo, S.C. Lim, D.J. Bae and Y.H. Lee, *J. Electrochem. Soc.*, **149**, A1058 (2002).
18. Q. Xiao and X. Zhou, *Electrochim. Acta*, **48**, 575 (2003).
19. V. Khomenko, E. Frackowiak and F. Beguin, *Electrochim. Acta*, **50**, 2499 (2005).
20. E. Frackowiak, V. Khomenko, K. Jurewicz, K. Lota and F. Beguin, *J. Power Sources*, **153**, 413 (2006).
21. B. Dong, B.L. He, C.L. Xu and H.L. Li, *Mater. Sci. and Eng. B*, **143**, 7 (2007).
22. S.R. Sivakkumar, W.J. Kim, J.A. Choi, D.R. MacFarlane, M. Forsyth and D.W. Kim, *J. Power Sources*, **171**, 1062 (2007).
23. J. Oh, M.E. Kozlov, B.G. Kim, H.K. Kim, R.H. Baughman and Y.H. Hwang, *Synth. Met.*, **158**, 638 (2008).
24. X. Lin and Y. Xu, *Electrochim. Acta*, **53**, 4990 (2008).
25. J.Y. Kim, K.H. Kim and K.B. Kim, *J. Power Sources*, **176**, 396 (2008).
26. S. Cosnier and M. Holzinger, *Electrochim. Acta*, **53**, 3948 (2008).
27. S. Paul and M. Joseph, *Sens. Actuators B*, **140**, 439 (2009).
28. C. Masarapu, H.F. Zeng, K.H. Hung and B. Wei, *ACS Nano*, **3**, 2199 (2009).
29. E. Frackowiak, S. Delpeux, K. Jurewicz, K. Szostak, D. Cazorla-Amoros and F. Beguin, *Chem. Phys. Lett.*, **361**, 35 (2002).